Electronic Supplementary Information

Impeller-like dodecameric water clusters in metal–organic nanotubes

Tien-Wen Tseng,*[a] Tzuoo-Tsair Luo,[b] and Kai-Hsiang Lu[a,b]

[a]Department of Chemical Engineering, National Taipei University of Technology, Taipei 106, Taiwan.
[b]Institute of Chemistry, Academia Sinica, Taipei 115, Taiwan.

1. Experimental section

Preparation of {[Cu(atc)(H_2O)]·H_2O}$_n$

Synthesis of **1**: Organic ligand 3-amino-1,2,4-triazole-5-carboxylic acid (H_2atc) (6.5 mg, 0.05 mmol) was completely dissolved in water (4 mL) that was then adjusted to pH = 9.0 by carefully adding 1.0 M potasium hydroxide solution, and put on the bottom of a test tube. Then, a methanol solution (v/v = 1:1, 10 mL) was layered on the former. Finally, $Cu(NO_3)_2 \cdot 3H_2O$ (6.1 mg, 0.025 mmol) was dissolved in MeOH (4 mL) and it was carefully layered on top. It was then allowed to stand at room temperature over a period of four weeks, whereupon green crystals of **1** were formed in 12% yield (0.7 mg, 0.003 mmol), based on Cu^{II}. Elemental analysis, found: C, 16.47; H, 2.71; N, 24.40. calcd for $C_3H_6CuN_4O_4$, {[Cu(atc)(H_2O)]·H_2O}: C, 15.97; H, 2.68; N, 24.83%; $C_3H_{5.7}CuN_4O_{3.85}$, {[Cu(atc)(H_2O)]·0.85H_2O}: C, 16.16; H, 2.58; N, 25.13 % (This is due to the intrinsic partial dehydration.)

Detailed reversible dehydration/rehydration studies

The existence of a wide plateau area in the TGA plot of **1** indicates that compound **1** would be amenable to a dehydration-rehydration study (Fig. S13). A freshly ground sample of **1** was heated at 110 °C for 1 h until a stable flat baseline of the TGA curve was observed, which indicates that all hosted water molecules were eliminated (weight loss about 15.2%, Fig. S15). The sample was then naturally cooled to room temperature by exposure to a moist atmosphere for 0.5 h. TGA analysis of the rehydrated samples (weight loss of water is about 15.2%, Fig. S15) reveals that the rehydration process is almost the same as that of as-synthesized. The water molecules were released without significant damaging the frameworks, as evidenced by the coincidence of the PXRD patterns of **1** sample heated to and held at 110 °C N_2 atmosphere with the patterns simulated from single-crystal structure. But the crystallinity of **1** could be recovered after rehydration. Furthermore, using the same sample, the cycle of dehydration/rehydration process can be repeated many times as monitored by PXRD (Fig. S16).

Crystal structure determination

{[Cu(atc)(H_2O)]·H_2O}$_n$ (1). A suitable single crystal of **1** with dimensions of 0.10 × 0.05 × 0.05 mm^3 was mounted on the tip of a glass fiber and placed onto the goniometer head for indexing and intensity data collection using a Nonius Kappa CCD diffractometer ($Mo_{K\alpha}$ = 0.71073 Å). The raw frame data for **1** were integrated into SHELX-format reflection files and corrected for Lorentz and polarization effects with the Denzo program.[1] An empirical absorption correction was applied by using the Multiscan method. The structure of **1** was solved by direct methods and refined against F^2 by the full-matrix least-squares technique, using the WINGX,[2] PLATON,[3] and SHELX[4] software packages. The non-hydrogen atoms were refined with anisotropic displacement parameters, and the hydrogen atoms of the framework were calculated and refined as riding modes. The hydrogen atoms of water molecules were found in difference Fourier maps but not refined. Crystal data for **1**: $C_3H_6CuN_4O_4\{[Cu(atc)(H_2O)]\cdot H_2O\}_n$, Mr = 225.66, rhombohedral, $R{-}3$, a = 21.5760(4) Å, b = 21.5760(4) Å, c = 8.9043(4) Å, γ = 120°, V = 3589.82(19) Å^3, Z = 18, ρ_{calcd} = 1.832 g cm^{-3}, μ = 2.721 mm^{-1}, λ (Mo$_{K\alpha}$) = 0.71073 Å, F(000) = 1960, T = 100(2) K, A total of 11346 reflections were collected in the range of $1.89° \leq \theta \leq 25.02°$, of which 1420 were unique (R_{int} = 0.0546). Final R indices: $R1$ = 0.0359, $wR2$ = 0.1044 for 1158 reflections [$I > 2\sigma(I)$]; $R1$ = 0.0472, $wR2$ = 0.1117 for 1420 independent reflections (all data) and 109 parameters, GOF = 1.067.

Magnetic study of compound 1

Variable temperature dependence of magnetic susceptibility of compound **1** was measured on powdered samples in the temperature range of 1.8–300 K at a 1.0 kG magnetic field.The plot of $\chi_M T$ versus T for **1** was shown in Fig. 3, indicating the magnetic susceptibility of compound **1** obeyed the Curie–Weiss law very well. The $\chi_M T$ value of **1** remained constant with decreasing temperature with a value of 2.57 emu K mol^{-1} from 300 to 70 K, but below it the $\chi_M T$ value decreased rapidly to 0.06 emu K mol^{-1} at 1.8 K. The spin-only value at 300 K was 2.57 emu K mol^{-1}, which is consistent with one magnetically isolated high-spin Cu(II) atoms with S = 1/2 exhibiting moderate spin–orbit coupling. The monotonic decrease in $\chi_M T$ with temperature is characteristic of compound **1** with overall antiferromagnetic interactions and/or spin–orbital coupling within **1**. The magnetic data can be analyzed using a Heisenberg Hamiltonian according to a simple six-J model. The spin Hamiltonian is given by:

$$H = -2J_1(S_1S_2) - 2J_2(S_2S_3) - 2J_3(S_3S_4) - 2J_4(S_4S_5) - 2J_5(S_5S_6) - 2J_6(S_6S_1),$$

Because the environmental of Cu1−Cu6 atoms are the same, thus, $J = J_1 = J_2 = J_3 = J_4 = J_5 = J_6$ (Fig. S18). The results of the fitting of the experimental data are shown as a solid line in Fig. 3, with final parameters being g = 2.1, J = − 33.7 cm^{-1}.

References

(1) Otwinowski, Z.; Minor, W. "*Processing of X-ray Diffraction Data Collected in Oscillation Mode*", *Methods in Enzymology*, Volume 276: Macromolecular Crystallography, part A, 1997, 307–326, Carter, Jr. C. W. and Sweet, R. M. Eds.,

Academic Press.

(2) Farrugia, L. J. *J. Appl. Crystallogr.*, 1999, **32**, 837.

(3) Spek, A. L. *J. Appl. Crystallogr.*, 2003, **36**, 7.

(4) Sheldrick, G. M. *SHELX-97*, University of Göttingen, 1997.

2. Figs. S1–S19

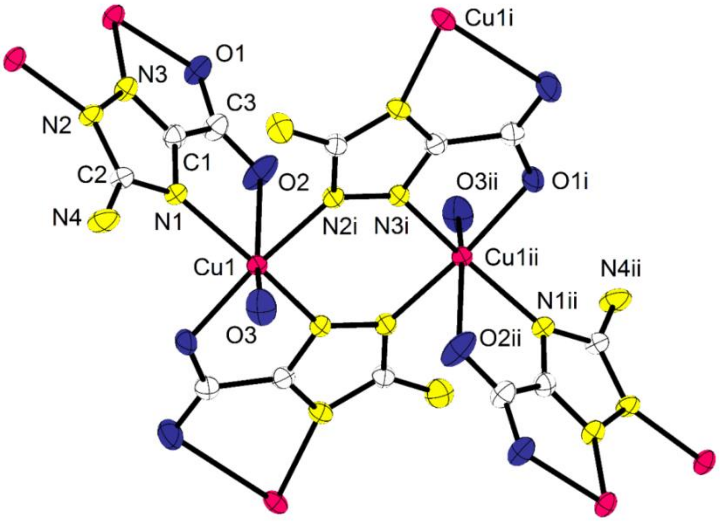

Fig. S1 The coordination environmental of Cu atoms in **1**. H atoms have been omitted for clarity (symmetry transformations used to generate equivalent atoms: i –y + 1/3, x – y + 2/3, z – 1/3; ii –x + 1/3, –y + 2/3, –z – 1/3).

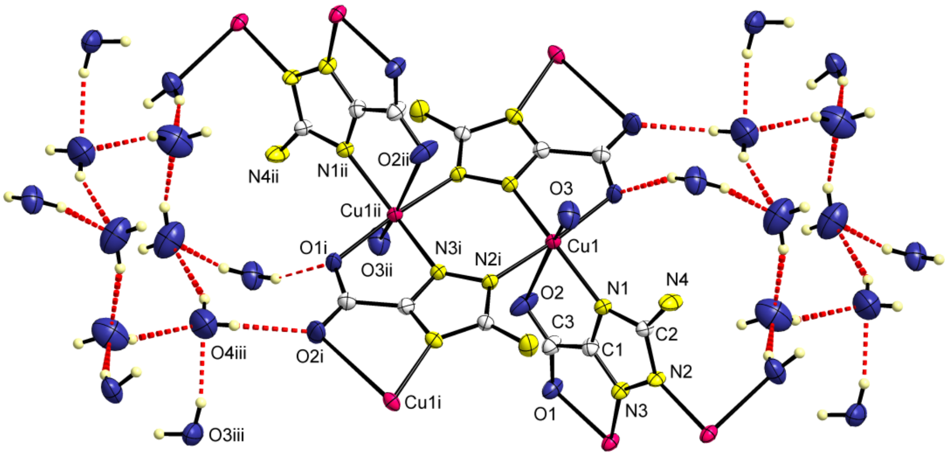

Fig. S2 The ORTEP drawing at 50% probability shows the guest hexameric water clusters are hydrogen-bonded to carboxylate motifs and coordinated water molecules (red = Cu, blue = O, yellow = N, light gray = C, pale yellow = H, red dotted line = H-bonding; symmetry transformations used to generate equivalent atoms: i –y + 1/3, x – y + 2/3, z – 1/3; ii –x + 1/3, –y + 2/3, –z – 1/3; iii y – 1/3, –x + y + 2/3, –z – 2/3).

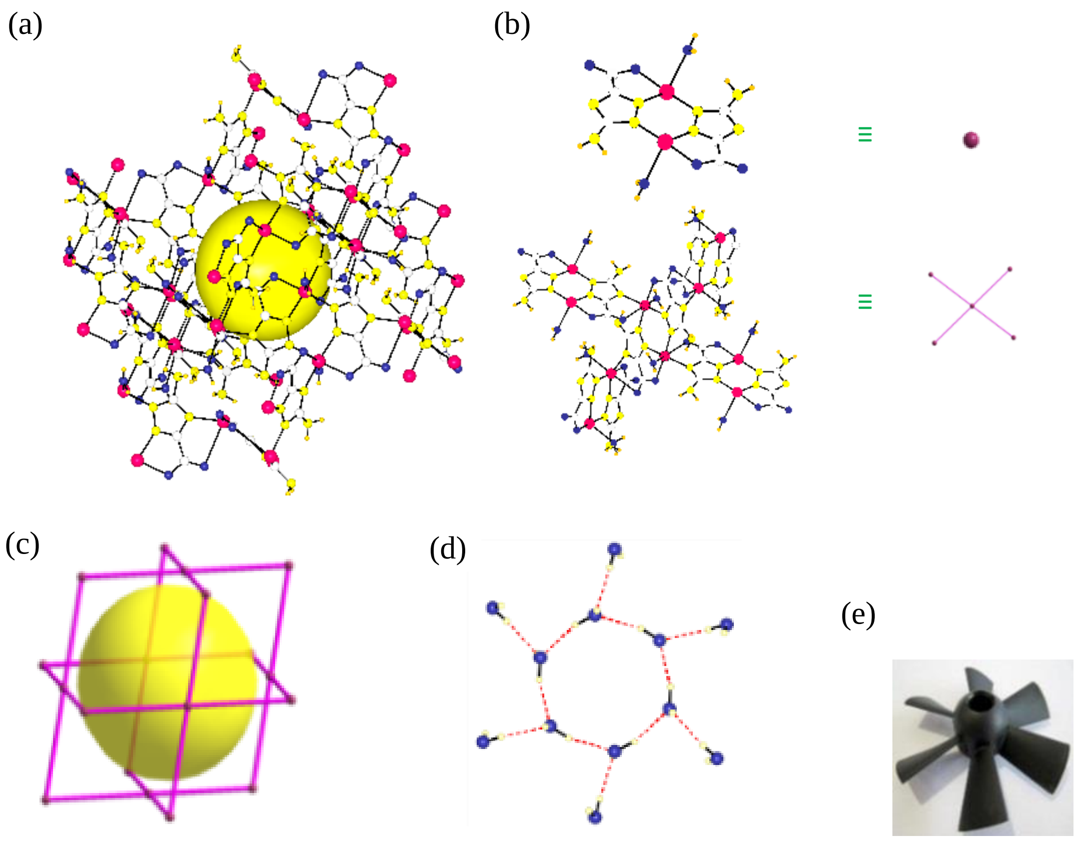

Fig. S3 The structures of **1**: (a) a 3D view shows the surrounding of the cavity, in which the water cluster was omitted for clarity; (b) a simplified framework; (c) an **nbo**-type topology; (d) a view of impeller-like dodecameric water cluster; (e) an image of impeller-like.

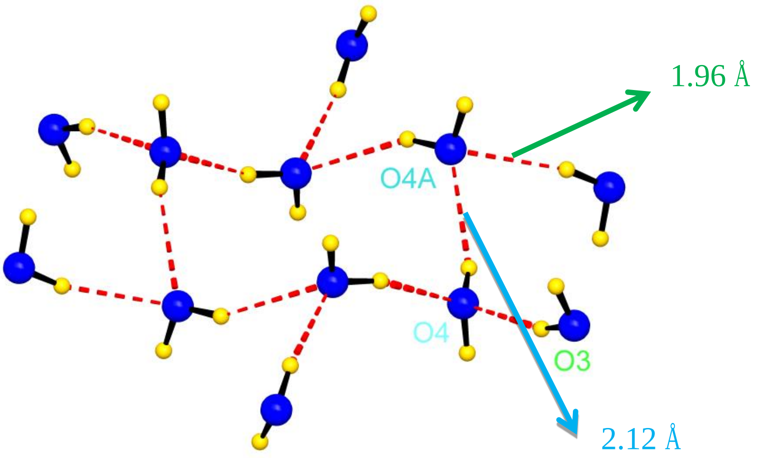

Fig. S4 Perspective view of $(H_2O)_{12}$, consists of six guest water (O4) linked into a core water cluster $(H_2O)_6$ that is further connected to six coordinated water (O3). Symmetry transformations used to generate equivalent atoms: A x – y + 2/3, x + 1/3, 1/3 –z.

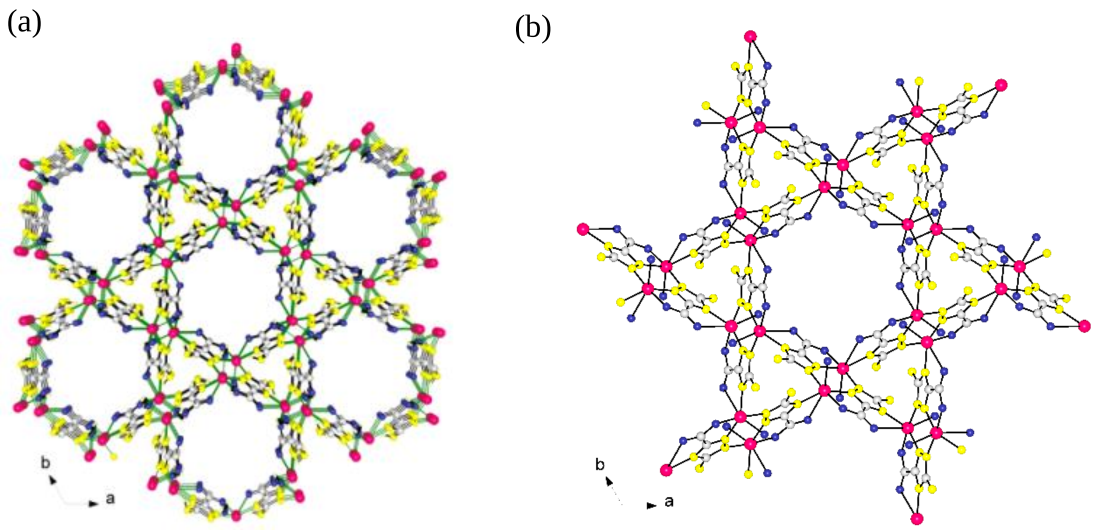

Fig. S5 (a) A view of **1** illustrates the motifs in the crystal structure with the ball and stick model along the *c* axis. (b) Top view of the tubular structure of **1**.

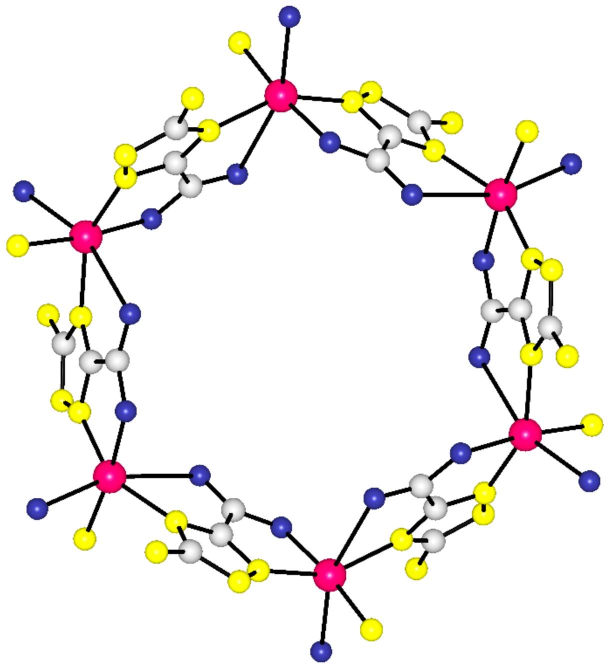

Fig. S6 A hexagonal channel is constructed by the Cu(II) ions and the bridging atc^{2-} ligands.

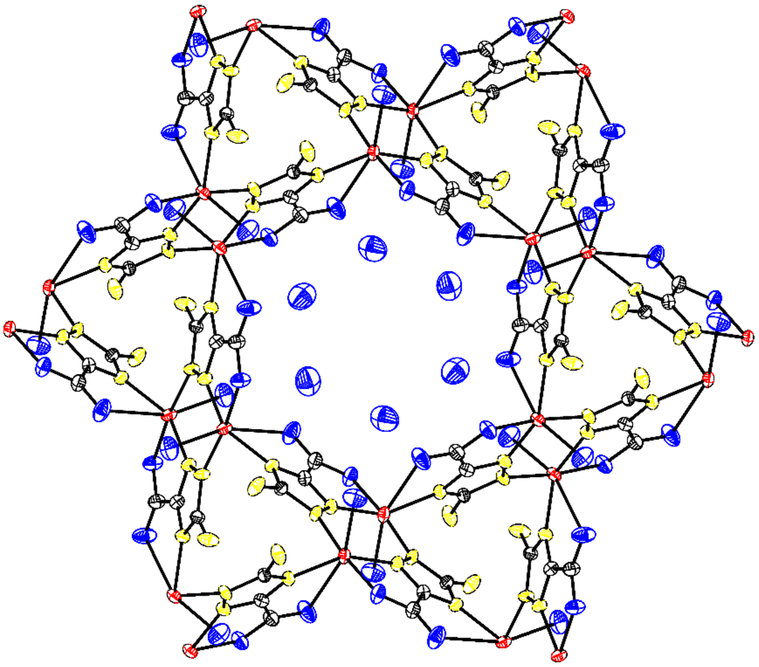

Fig. S7 Top view of the trapped guest water cluster included within a channel.

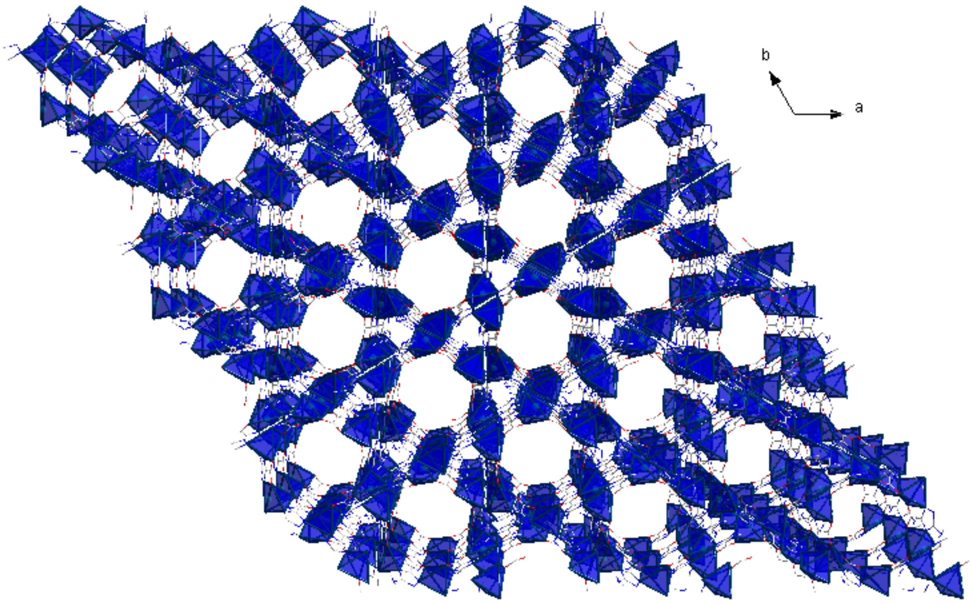

Fig. S8 A packing diagram of **1** viewed along the *c* axis, shows the bridging atc^{2-} ligands bind the copper metal centers, which are highlighted in a blue distorted octahedral.

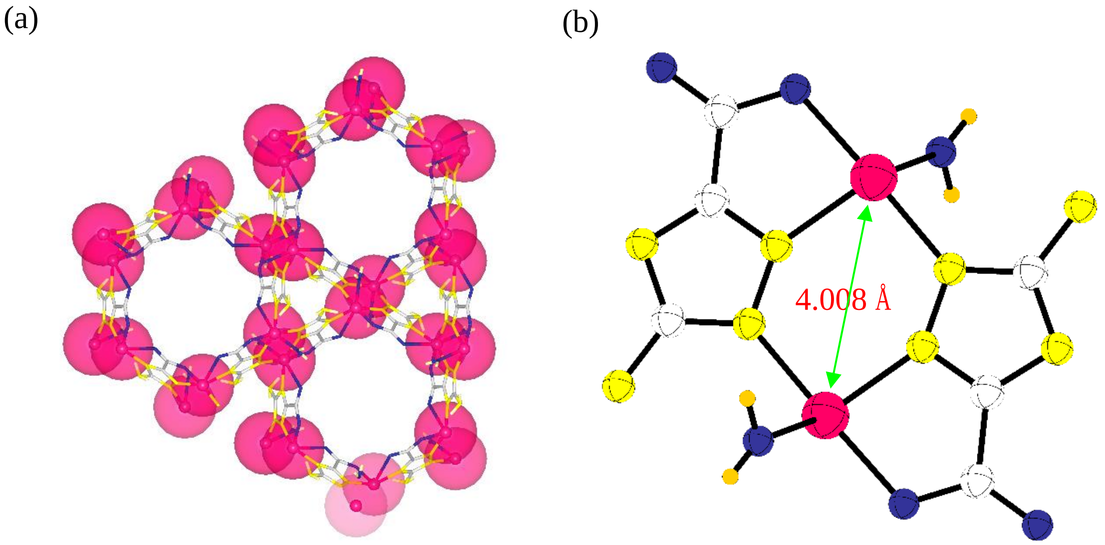

Fig. S9 The structure of **1**: (a) top view of hexagonal channels; (b) each corner of channels is comprised of two Cu(II) centers and two bridged atc^{2-} ligands with a separated distance of 4.008 Å .

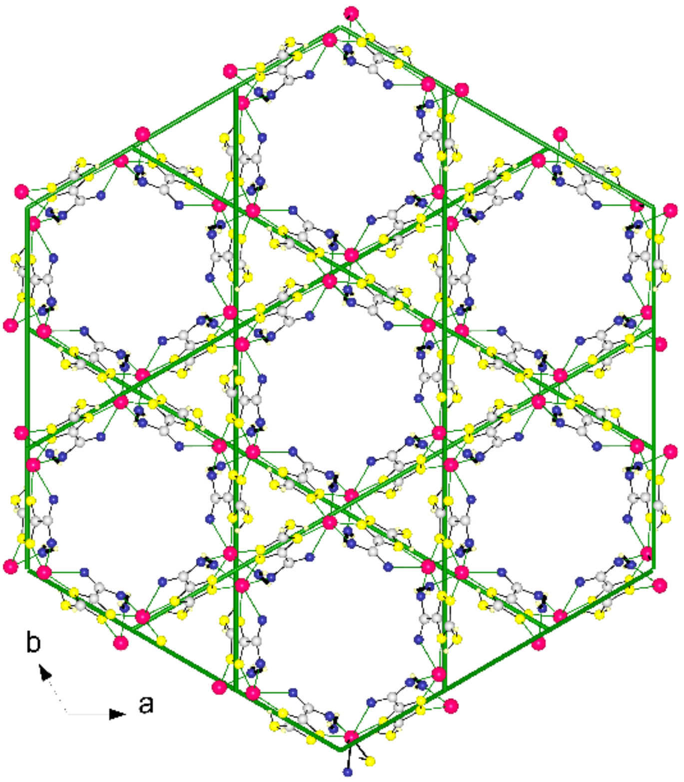

Fig. S10 Top view of the framework of **1** along the *c* axis.

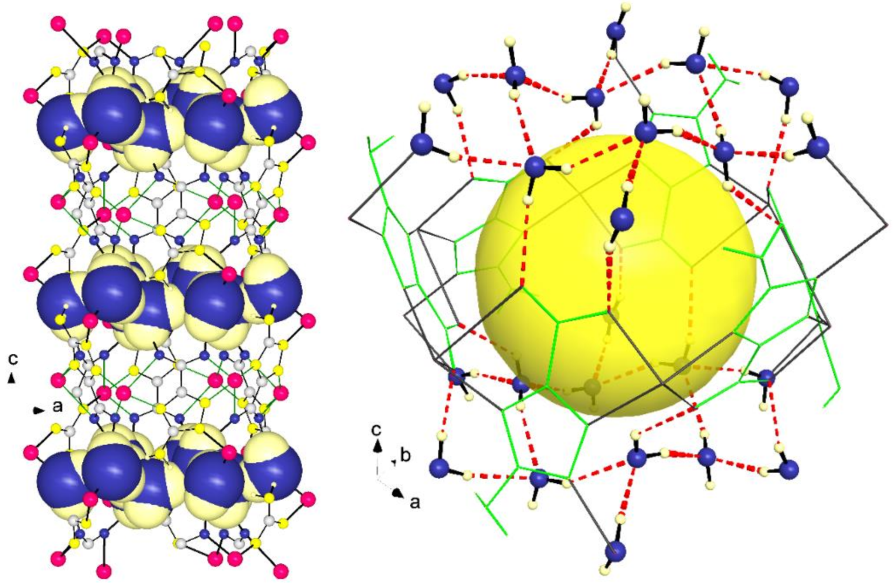

Fig. S11 Perspective view of the dodecameric water clusters of **1** with a space-filling mode (left); a tubular cavity highlighted in a yellow ball (right).

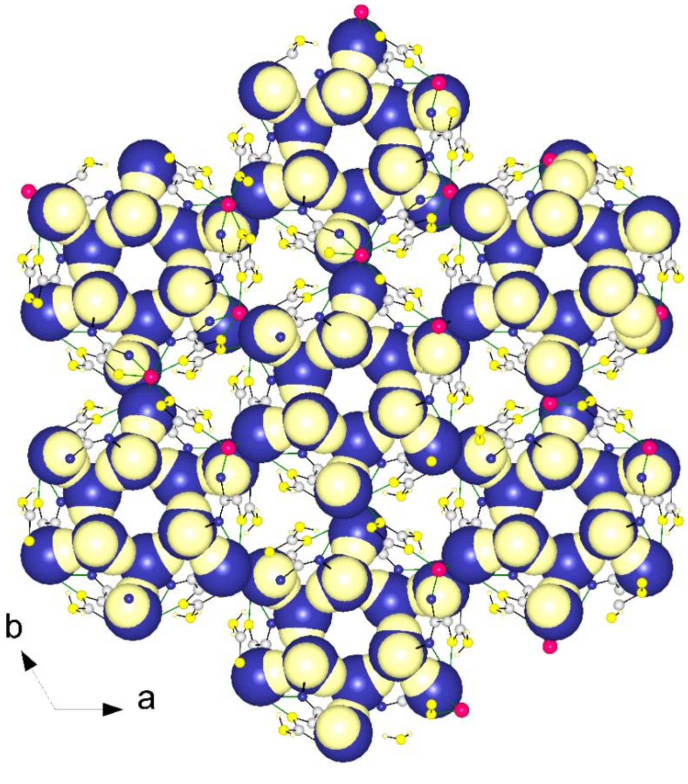

Fig. S12 Perspective view of the dodecameric water clusters in the space-filling mode of **1**.

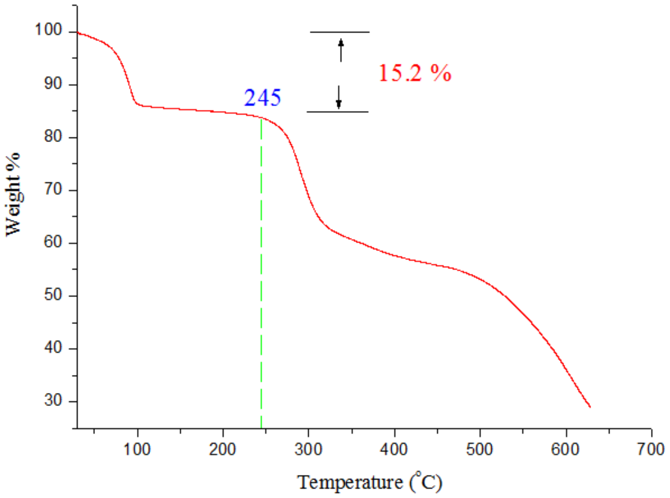

Fig. S13 Thermogravimetric analysis (TGA) curve of compound **1**.

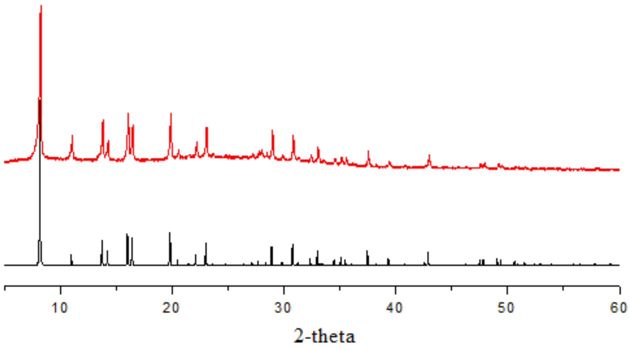

Fig. S14 Powder X-ray diffraction (PXRD) patterns of **1** (as-synthesized, red; simulated, black).

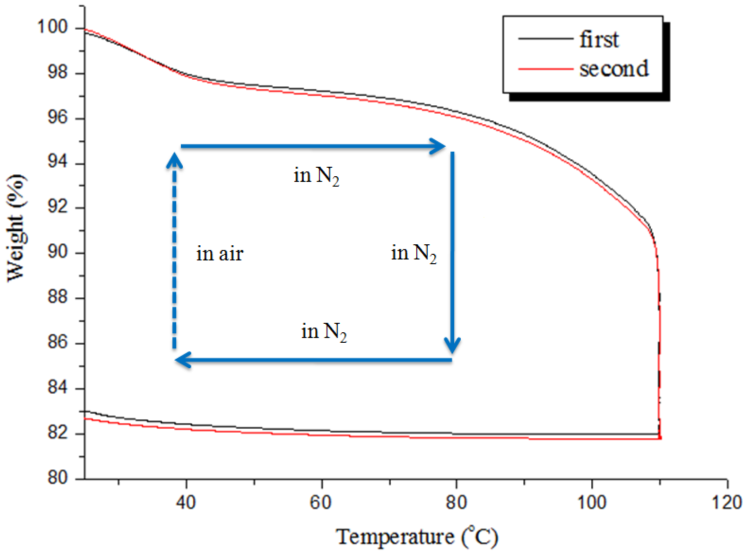

Fig. S15 Compound **1** was dehydrated at 110 ℃ for 1 h and exposed to moist atomsphere for 0.5 h at room temperature (black: first round; red: the second round).

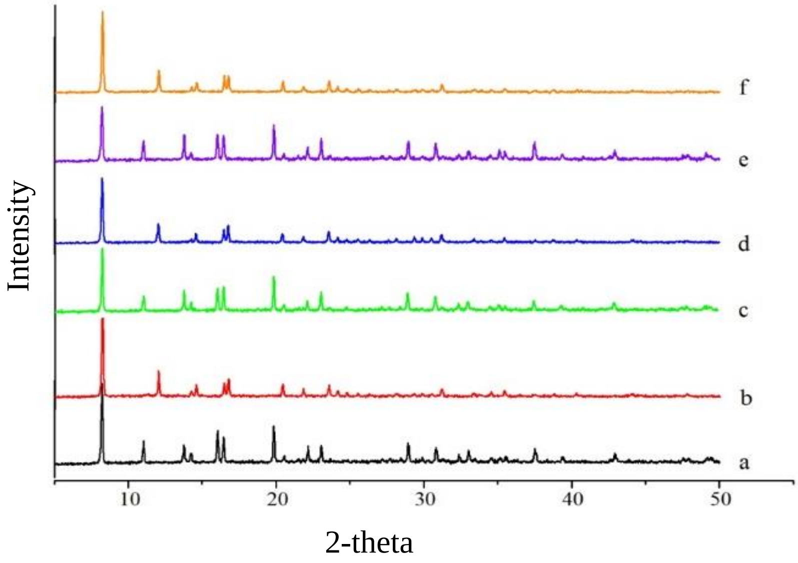

Fig. S16 Comparison of the PXRD patterns of **1**, (a) as-synthesized (RT), and (b)−(f): three reversible cycles of dehydration (1 h, 110 ℃) and rehydration (0.5 h, at RT).

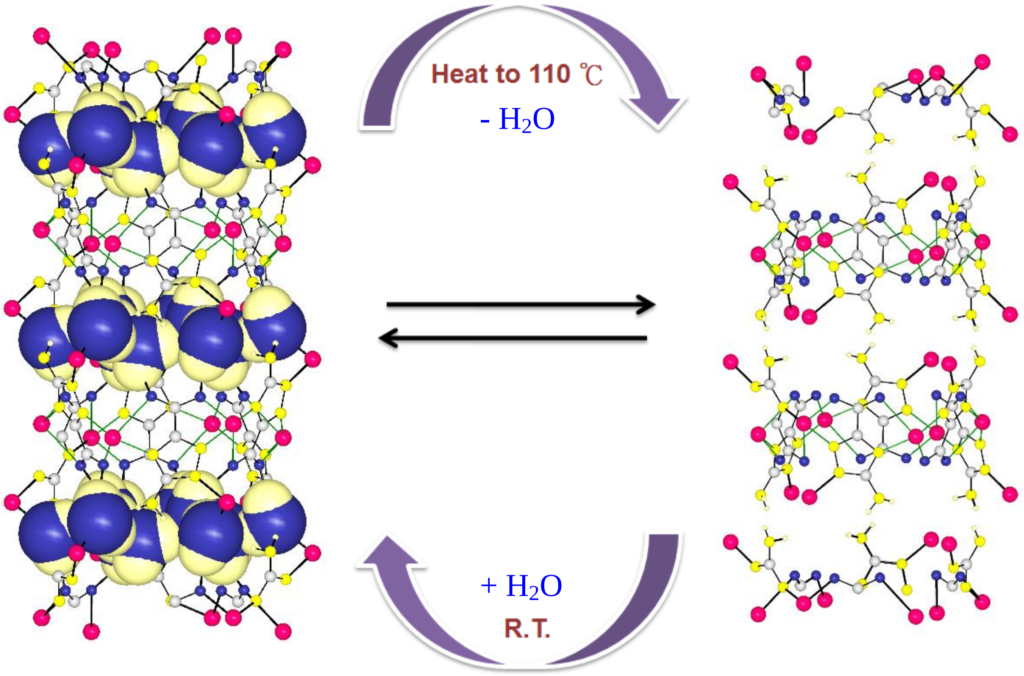

Fig. S17 Schematic view shows the reversible dehydration and rehydration processes of water molecules in a nanotubular framework of **1**.

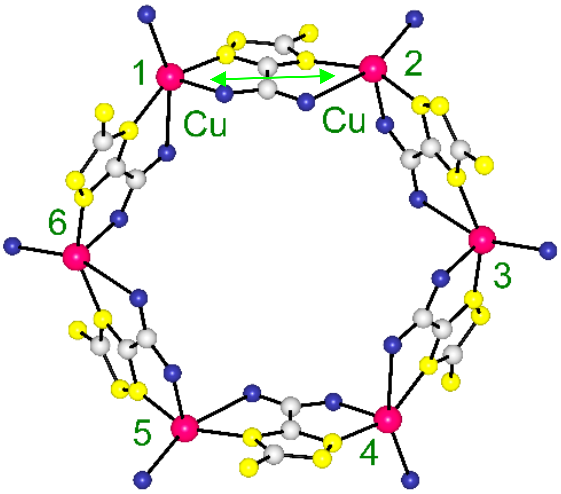

Fig. S18 Showing the spin–orbital coupling within **1** with 6-J model ($J = J_1 = J_2 = J_3 = J_4 = J_5 = J_6$).

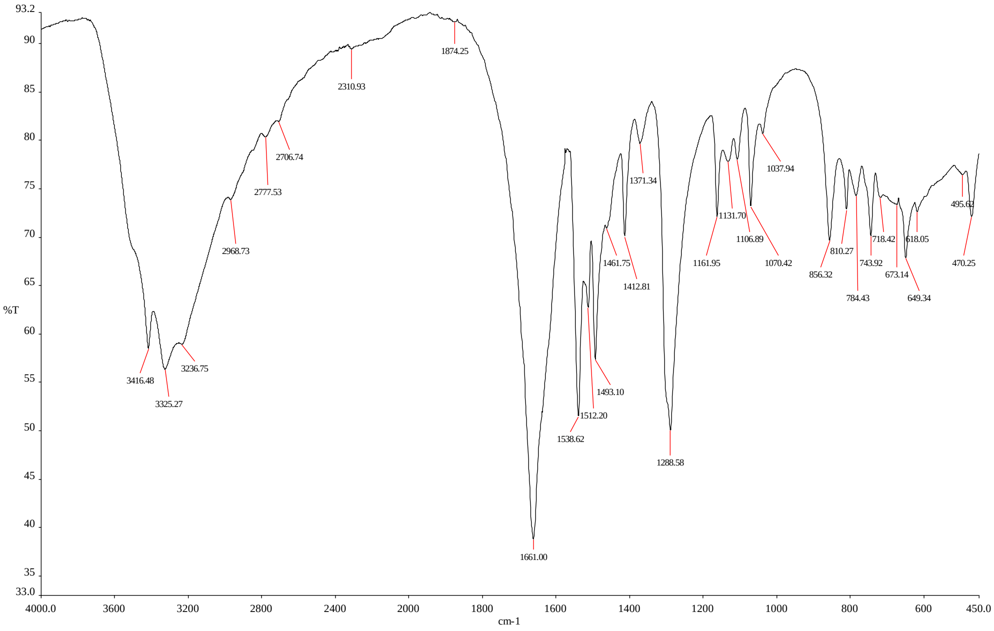

Fig. S19 IR spectrum of compound **1**.

3. Tables S1–S3

Table S1. Crystal Data and Structure Refinement for Compound **1**

Empirical formula	$C_3H_6CuN_4O_4$	
Formula weight	225.66	
Temperature	100(2) K	
Wavelength	0.71073 Å	
Crystal system	Rhombohedral	
Space group	R–3	
Unit cell dimensions	a = 21.5760(4) Å	α = 90°
	b = 21.5760(4) Å	β = 90°
	c = 8.9043(4) Å	γ = 120°
Volume	3589.82(19) Å ^{3}	
Z	18	
Density (calculated)	1.832 Mg/m^3	
Absorption coefficient	2.721 mm^{-1}	
F(000)	1960	
Crystal size	0.1 x 0.05 x 0.05 mm^3	
Theta range for data collection	1.89 to 25.02°	
Index ranges	-25<=h<=25, -25<=k<=25, -10<=l<=10	
Reflections collected	11346	
Independent reflections	1420 [R(int) = 0.0546]	
Completeness to theta = 25.02°	100.0 %	
Absorption correction	Semi-empirical from equivalents	
Max. and min. transmission	0.7452 and 0.6742	
Refinement method	Full-matrix least-squares on F^2	
Data / restraints / parameters	1420 / 0 / 109	
Goodness-of-fit on F^2	1.067	
Final R indices [I > 2 sigma(I)]	R_1 = 0.0359, wR_2 = 0.1044	
R indices (all data)	R_1 = 0.0472, wR_2 = 0.1117	
Largest diff. peak and hole	1.104 and -0.378 e.Å $^{-3}$	

Table S2. Selected Bond Lengths [Å] and Angles [°] for Compound **1**

Cu(1)-N(2)#1	1.977(3)	N(3)#2-Cu(1)-O(3)	109.28(14)
Cu(1)-N(3)#2	1.996(3)	O(1)#2-Cu(1)-O(3)	89.49(13)
Cu(1)-O(1)#2	1.998(3)	N(1)-Cu(1)-O(3)	98.28(14)
Cu(1)-N(1)	2.017(3)	C(3)-O(1)-Cu(1)#3	115.4(3)
Cu(1)-O(3)	2.313(3)	C(2)-N(1)-Cu(1)	139.8(3)
N(2)#1-Cu(1)-N(3)#2	95.73(14)	C(1)-N(1)-Cu(1)	117.3(3)
N(2)#1-Cu(1)-O(1)#2	173.61(14)	C(2)-N(2)-Cu(1)#4	132.5(3)
N(3)#2-Cu(1)-O(1)#2	81.47(13)	N(3)-N(2)-Cu(1)#4	121.3(2)
N(2)#1-Cu(1)-N(1)	94.97(14)	C(1)-N(3)-Cu(1)#3	110.8(3)
N(3)#2-Cu(1)-N(1)	151.01(14)	N(2)-N(3)-Cu(1)#3	140.9(3)
O(1)#2-Cu(1)-N(1)	90.16(13)		
N(2)#1-Cu(1)-O(3)	86.00(14)		

Symmetry transformations used to generate equivalent atoms:

#1 -y+1/3, x-y+2/3, z-1/3 #2 y, -x+y, -z #3 x-y, x, -z

#4 -x+y-1/3, -x+1/3, z+1/3

Table S3. The Hydrogen Bonding Distances (Å) and Angles (°) for Compound **1**

D–H···A (Å)	**D–H (Å)**	**H···A (Å)**	**D···A (Å)**	**D–H···A (^{o})**
O3–H3B···O4	0.83	1.96	2.768(7)	164
O4–H42···O4	0.85	2.12	2.900(5)	154
O4–H41···O2	0.85	2.15	2.800(6)	133